



Electroless Ni-P Plating of Carbon Steel via Hot Substrate Method and Comparison of Coating Properties with those for Conventional Method

P. Verdi and S.M. Monirvaghefi

Submitted: 13 December 2019 / Revised: 1 October 2020 / Accepted: 11 October 2020 / Published online: 20 November 2020

In this study, Ni-P electroless coating was deposited on carbon steel by a new method called SLHS (substrate local heating system) which makes a higher rate of deposition possible without the risk of decomposition of electroless baths. The effects of pH and temperature on plating rate, composition, surface morphology, hardness and corrosion of the coating in SLHS condition ($T_{\text{sub}} = 190\text{ }^{\circ}\text{C}$, $T_{\text{bath}} = 80\text{ }^{\circ}\text{C}$) were investigated. In addition, the impact of heat-treatment at $400\text{ }^{\circ}\text{C}$ for 1 h on hardness, morphology and microstructure was also studied. Samples prepared by this method were characterized by Scanning Electron Microscopy/Energy-Dispersive x-ray analysis, Light Microscope and x-ray diffraction. They were then submitted to Vickers microhardness and tribological tests. The deposition rates of electroless nickel (EN) coating were first estimated by weight gain method and then by light and scanning electron microscopy. Electrochemical Impedance Spectroscopy (EIS), Tafel polarization and salt spray tests were then used to evaluate the corrosion properties of the coatings. The study shows that maximum deposition rates for conventional and SLHS samples were approximately $20\text{ }\mu\text{m/h}$ and $32\text{ }\mu\text{m/h}$, respectively. This increase in the plating rate reduces the phosphorus level by nearly 1.5 wt.% for SLHS sample. The corrosion resistance of SLHS sample is improved in comparison to the conventional one.

Keywords carbon steel, corrosion, electroless, heat treatment, hot substrate, nickel-phosphorus coating

1. Introduction

Plating can generally be classified into two categories, namely electrical and chemical. The electroless process is a chemical coating technique in which there is a deposition of a metal, an alloy, or a composite on an activated surface by autocatalytic reduction of metallic ions from a salt solution containing a reducing agent (Ref 1). It is well known that electroless plating is an effective method for increased corrosion resistance and anti-wear properties of materials (Ref 2). Some of the advantages of using electroless coating are uniformity, excellent corrosion resistance, wear and abrasion resistance, solderability, high hardness, self-lubrication, increased hardness after heat-treatment, ability to plate irregular shapes and capability of depositing thin films of metal on nonconducting surfaces (e.g., glass, ceramics, polymers) (Ref 3). While there are many advantages to electroless plating, there

are some disadvantages as well. Problems like a low rate of deposition, hazardous plating solutions, need for accurate control of chemicals, temperature and pH, detrimental by-product generation, limited bath life and higher operating cost must be considered for electroless plating (Ref 3, 4).

For the electroless process, the deposition conditions, such as bath composition, plating temperature, pH, bath stirring, plating period, stabilizer and additives could have a significant impact on the deposition rate (Ref 5). Among these, temperature and pH have a tremendous effect on both the deposition rate and phosphorus content of the electroless film. Generally, the Ni formation reaction is faster than the P formation reaction. When the pH of the solution is reduced, the P formation reaction speeds up and the Ni formation reaction slows down. Therefore, pH reduction leads to lower precipitation of Ni-P and an increment in P in the coating (Ref 6).

In the case of temperature, the deposition rate is increased with increasing bath temperature, and inversely the phosphorus content is decreased when using higher temperatures. The EN coating process is based on a redox reaction in which a reducing agent is oxidized, and Ni^{2+} ions are reduced on the surface of the substrate materials (Ref 7). This process needs a proper temperature to provide sufficient energy for reactions. Low temperatures offer a reduced amount of energy to the reaction which as well leads to poor deposition rates. Very high temperatures, on the other hand, could make the bath excessively active, probably ensuing in plate-out and general bath unsteadiness (Ref 4). For the weak acidic electroless baths with nickel sulfate as a nickel source and sodium hypophosphite as a reducer, temperatures between 85 and $92\text{ }^{\circ}\text{C}$ are recommended, although $90\text{ }^{\circ}\text{C}$ is more common in the literature, because of more stability (Ref 8, 9). In recent years, considerable efforts have been expended to raise the

P. Verdi, Materials Engineering Group, Pardis College, Isfahan University of Technology, Isfahan 84156-83111, Iran; and S.M. Monirvaghefi, Department of Materials Engineering, Isfahan University of Technology, Isfahan 84156-83111, Iran. Contact e-mail: p.verdi@pa.iut.ac.ir.

Table 1 Catalytic activity of metals and materials as a substrate for nickel electroless plating

A-Material with Inherent catalytic activity	B-Material with nonInherent catalytic activity
I: including Co, Ni, Rb, Pa, Ir and Pt	II: metals with nobility < Ni including Fe, Al, Be, Ti III: metals with nobility > Ni including Cu, Au, Ag, C IV: nonmetallic including polymers and ceramic

rate of electroless plating and make the process more economical. Since controlling the bath stability above 90 °C is very difficult and the bath solution decomposition happens, the rate of deposition is usually limited to maximally 20 μm/h. In addition, in such high temperature, the bath solution is severely evaporated.

The surfaces of ceramic, glass, passivated stainless steel or passivated titanium heaters used in the industrial electroless bath have a high temperature exceeding 400 °C, which is an interesting point. In this situation due to the non-catalytic nature of heaters and suitable circulation of the bath, plating out does not happen. In general, according to Table 1, the catalytic activity of metals and material as a substrate in nickel electroless plating can be sorted into two main categories (A-B) or four divisions (I-IV).

Recently, some researchers have reported the effect of temperature modification on the electroless method. Cobley et al. introduced a new method called ultrasonically enabled low-temperature electroless plating and showed that for electroless copper plating, the temperature operation (30-70 °C) can be lowered with the aid of ultrasonic waves. This technique can reduce energy usage, and manufacturing costs, and can improve sustainability (Ref 10). Anvari used a glass reactor to indirectly warm up the electroless bath with hot water, and by accurately changing the temperature and pH, the FGC (Functionally Graded Coating) structure including high, medium and low phosphorus layers were obtained (Ref 11). Karthikeyan et al. (Ref 12) indirectly heated electroless solution in a beaker with a hot oil system and by using a hot plate to keep the oil temperature at 87 °C. Gao et al. proposed applying the constant current to electroless plating called electrochemically promoted electroless plating, in order to decrease the temperature of the electroless plating while keeping enough deposition rate. The operating temperature of the electroless plating nickel-phosphorous coating on Ti substrate is decreased to 40-60 °C due to the electrochemical promotion (Ref 13). Sung et al. patented a novel electroless process called non-isothermal deposition in which heating a plating solution located a gap between the heating device and a target resulting in a higher rate of deposition. The cooling device (a condenser) can maintain the low temperature of the plating bath in a non-reaction area and take the extra heat energy away. Therefore, although the substrate temperature reached near 180 °C, the bulk temperature can remain at 60 °C without deteriorating the plating bath (Ref 14-20).

In this study, a new method called SLHS (substrate local heating system) is introduced that can increase the deposition rate without the previously mentioned problems. In this process, a steel substrate with catalytic surface warms up to 190 °C, while bath temperature is kept around 80 °C. The properties of the SLHS electroless coating is evaluated and compared with the conventional one.

2. Materials and Methods

For this experiment, AISI 1045 carbon steel disks with 25 mm diameter and 5 mm thickness with a composition of 0.46% C, 0.83% Mn, 0.26% Si, 0.07% Cr, 0.02% Mo, 0.02% P were used as substrates. The samples were ground (from 600 up to 1200 grind size SiC paper) and polished with Al₂O₃ suspension. Prior to the plating process, the surfaces of all the samples were ultrasonically cleaned by acetone for 10 min and then were degreased by immersion in NaOH solution for 15 min at 40 °C. Finally, the sample surfaces were activated in HCl 30% for 30 s. Rinsing in deionized (DI) water between each step is necessary. A commercial electroless nickel bath (SLOTONIP 70A from Schlotter) with a hypophosphite reducer was used in order to deposit Ni-P layers. The pH was varied between 4.6 and 5.2 and controlled by adding ammonia and H₂SO₄ acid. A benchmark pH meter model AZ 86505 was used to determine the pH of the solution. The condition of the plating bath for conventional and SLHS methods is shown in Table 2.

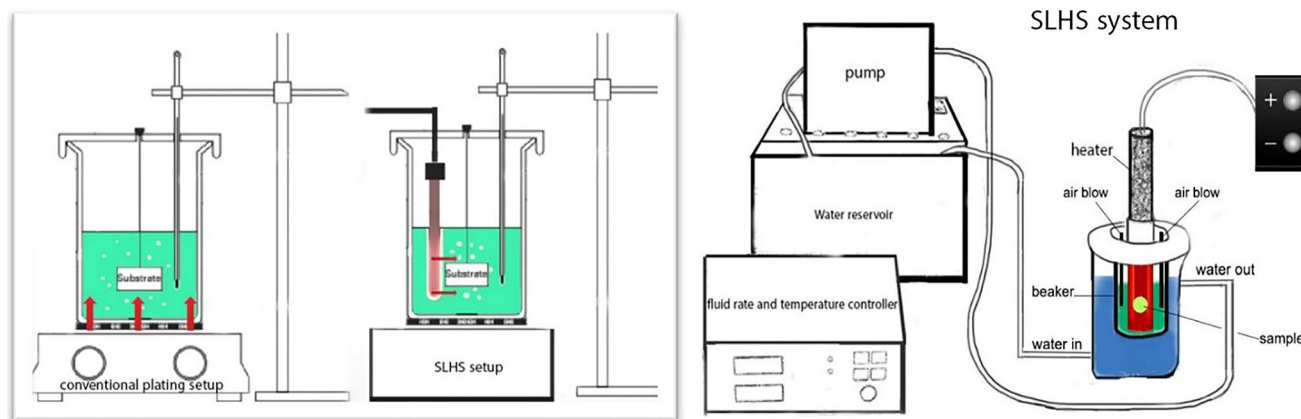
The schematic illustrations of SLHS and conventional plating methods are shown in Fig. 1. The heating system for them is totally different. For comparison, two series of samples were prepared. For Series 1, the substrates were normally coated by a mini heat-air stirring system. The maximum plating rate obtained for these groups is 20 μm/h. For Series 2, the samples were plated by SLHS system in which the solution was warmed by an elemental resistance heater at 1000-watt, and the air was used as a stirring-coolant of the solution. The temperatures of the bath, stainless-steel tube and substrate were measured with an alcoholic thermometer, a thermocouple and an infrared thermometer, respectively. The results of these measurements are shown in Table 3.

In order to cool down the solution and keep the temperature below the critical temperature that results in a hot spot, plate out and decomposition, a simple rotation of fluid system including a pump and cold-water reservoir was used (Fig. 1).

Thickness measurement of the coated samples was done by weight gain method, digital micrometer, SEM and OM, the thermal simulation of SLHS system was done utilizing the Abaqus and COMSOL software, and the simulation process is defined by six temperature nodes according to Table 3. The surface morphologies of NiP coatings in both plating methods were investigated using Field Emission Scanning Electron Microscopy (FE-SEM, MIRA3 TESCAN-XMU), SEM (ZEISS) and Optical microscopy (Olympus). The chemical composition of coatings was analyzed by EDX systems attached to Scanning Electron Microscopy (SEM). In addition, crystallization and phase transformation behavior of electroless nickel-phosphorus deposits after heat treatment were studied by an XRD instrument model XPERT using Cu Kα target, and the microhardness test was carried out using Micro Vickers Hardness Tester, model Metalux, by subjecting the samples to a

Table 2 Plating condition for conventional and SLHS methods

Condition	Conventional plating	SLHS plating
Bath solution	SLOTONIP 70A	SLOTONIP 70A
Stirring method	Air agitation	Air agitation
pH	4.6-5.2	4.6-5.2
Temperature	90 °C (solution)	190 °C (substrate), 80 °C (solution)
Cooling system	No	exterior water circulation with air injection in solution
Time of deposition	1 h	1 h

**Fig. 1** Schematic illustration of conventional and SLHS electroless plating**Table 3** Result of temperature measurement in different zones of the SLHS system

Heating zone	Temperature, average
Heater surface (for heating of substrate)	450 °C
Quartz glassy tube (for insulation of heater and solution)	390 °C
The gap between the glassy tube and a stainless-steel tube	320 °C
Substrate	190 °C
Solution near heater	95 °C
Solution near the end of a beaker	80 °C

load of 25 g during 10 s in as-plate and after the heat treatment condition. The hardness test results are based on an average of five indentations.

For corrosion evaluation, salt spray, Tafel polarization and EIS (electrochemical impedance spectroscopy) tests were conducted. Salt spray tests were carried out in 5 wt.% NaCl solution at 35 °C according to the ASTM B117 standard. Tafel polarization tests in 3.5 wt.% NaCl solution were executed with the aid of Potentiostat model PARSTAT 2273 to measure corrosion rates. The applied potential range was ± 250 mV with respect to OCP potential with a scan rate of 1 mV/s. For analysis of the data curve and corrosion parameters, the PowerSuite software was used. Before the test, the OCP condition was established. In addition, the corrosion behavior of coatings was studied by EIS technique in 3.5 wt.% NaCl solution. A conventional three-electrode cell which consists of an electroless plated sample as the working electrode, an Ag/AgCl as a reference electrode, and a platinum rod as a counter electrode, was used for that. The measurements were carried out by applying a sine wave with an amplitude of 10 mV over a frequency range between 0.01 Hz and 10 kHz.

3. Results and Discussion

The SLHS method was based on increasing the substrate temperature instead of the bulk of solution temperature. The idea comes from the fact that a substrate surface is a favorable place for chemical reactions to occur. Therefore, if the bath solution is cooling down at least 10 °C below the typical bath temperature (90 °C) and then substrate temperature reaches near 200 °C, the bath can work with the rate of over 30 $\mu\text{m/h}$, and without the risk of decomposition. The successive key is ensuring that the solution temperature never exceeds the critical value by various techniques such as injecting cool air into the bath. The SLSHS electroless plating method has many advantages such as saving plating time and the possibility of local plating of the parts over the conventional approach.

3.1 Rate of Deposition

The effect of plating temperature on the thickness of Ni-P film produced by both conventional and SLHS methods was studied. The plating rate was measured after plating in coated

samples first via weight gain method $R = (\Delta w \times 60 \times 10000) / (d \times A \times t)$ (Ref 25) where Δw is the differences between the weight of samples before and after plating (with the accuracy of 0.01 g), d represents the density of electroless coating ($\sim 7.9 \text{ g/cm}^3$), A stands for a sample surface area (cm^2) and t shows the time of deposition (min). By using a digital scale with an accuracy of 0.01 gr, all samples' weights were recorded before and after the plating for 1 h. Secondly, thickness measurement is carried out by means of a digital micrometer before and after plating. Finally, the sample cross section is studied by SEM and LM for precious thickness measurement.

Concerning bath stability, for conventional plating, the plating rate maximally reached $20 \text{ }\mu\text{m/h}$ in $\text{pH} = 5$ and $T_{\text{solution}} = 90 \text{ }^\circ\text{C}$ (Fig. 2). Otherwise, the coating thickness maximally reached $32 \text{ }\mu\text{m/h}$ in $\text{pH} = 5.2$ and $T_{\text{sub}} = 190 \text{ }^\circ\text{C}$ by SLHS technique (Fig. 2). Since high deposition rate is in contrast to bath stability, using pHs such as 5.1 for conventional and 5.3 for SLHS samples causes hot spots and decomposition of the solution at such a high temperature. Technically, an increase in both pH and temperature parameters can boost the plating rate, but this increase is limited to certain values because the bath works well only when it is sufficiently stabilized. When the temperature of the bath solution exceeds $95 \text{ }^\circ\text{C}$, the solution is suddenly decomposed and forms a black deposit. Therefore, in SLHS method, the temperature of the solution must be at least $10 \text{ }^\circ\text{C}$ below $90 \text{ }^\circ\text{C}$ in order to maintain the bath stability. In other words, when the substrate in the center has a high temperature (near $190 \text{ }^\circ\text{C}$), the solution in the outer zone of the solution must be cool enough (near $80 \text{ }^\circ\text{C}$) to make the SLHS approach working. Obviously, the volume of the heating zone near the sample is much smaller than the bath bulk volume. Furthermore, using cold water continuously pumped around the glass beaker can keep the temperature low enough. For the solution near the sample, with the aid of two air tubes, the temperature would not exceed $95 \text{ }^\circ\text{C}$. Figure 3 and 4 shows the result of thickness measurement for 1 h in both conventional and SLHS methods via SEM and light microscopy.

The plots of deposition rate versus increasing substrate temperature in various pHs for SLHS method are shown in Fig. 5.

The plots of phosphorus content versus pH at different substrate temperatures for SLHS method are shown in Fig. 6.

Now it is time to explain the possible reasons for this improvement in plating rate. As previously mentioned, the deposition rate can change by temperature and pH variation. According to cathodic reaction $\text{Ni}^{2+} + 2\text{e}^- = \text{Ni}^0$ and anodic

reaction $\text{H}_2\text{PO}_2^- + \text{H}_2\text{O} = \text{H}_2\text{PO}_3^- + 2\text{H}^+ + 2\text{e}^-$ that briefly form the overall reaction: $\text{Ni}^{2+} + \text{H}_2\text{PO}_2^- + \text{H}_2\text{O} = \text{H}_2\text{PO}_3^- + 2\text{H}^+ + \text{Ni}^0$, electroless plating includes redox reactions. Although, other cathodic reactions in the electroless bath such as $\text{H}_2\text{PO}_2^- + 2\text{H}^+ + \text{e}^- \rightarrow \text{P} + 2\text{H}_2\text{O}$ and $2\text{H}^+ + 2\text{e}^- \rightarrow \text{H}_2$ also exist. These kinds of reactions are usually endothermic and need thermal energy. Therefore, by increasing the temperature, the reactions can occur more rapidly.

The second reason can be defined with the electrical double layer model. The double-layer is simply the arrangement of charges in the interface between the sample surface and electrolyte. In his book, Riedel introduced the model that is composed of two different layers called Helmholtz and diffusion (Ref 21). By boosting up the temperature, the thickness of the diffusion layer is decreased and the rate of diffusion is increased. By proceeding with the plating, the pH of the bath around the substrate becomes lower, but by contacting the diffusion layer with the bulk solution, this drop-off in the pH is compensated. As a result, the rate of deposition is increased.

The last reason is related to the kinetics of electroless plated Ni-P alloy film. In general, the growth rate of the electroless plated Ni-P alloy film, is an exponential function of the plating temperature, $T(\text{K})$, that can be expressed as $v = k \exp[-E_a/RT]$ in the unchangeable concentration condition (Ref 5), where E_a , k , R and T are activation energy, rate constant, gas constant ($8.314 \text{ J mol}^{-1} \text{ K}^{-1}$) and temperature, respectively. If the concentration value is not fixed during the process, the following equation will be used: $v = dc/dt = k[\text{Ni}^{2+}][\text{H}_2\text{PO}_2^-][\text{H}^+][\text{H}_2\text{PO}_3^-][\text{L}][\text{A}] \exp[-E_a/RT]$ (Ref 5), where: $[\text{Ni}^{2+}]$ is the concentration of nickel ion, $[\text{H}_2\text{PO}_2^-]$ shows the concentration of hypophosphite ion, $[\text{H}^+]$ represents the concentration of hydrogen ion, $[\text{H}_2\text{PO}_3^-]$ stands for the concentration of orthophosphate ion and L and A depict the concentration of complexing agents and accelerator, respectively. By taking the logarithm of the last equation, E_a can be obtained from the slope of plot $\log(v)$ versus $1/T$ in the form of $E_a = 2.3(8.314 \text{ J mol}^{-1} \text{ K}^{-1})$ (slope).

According to Lin and Long (Ref 22), the activation energy (E_a) mainly refers to that for growth, not for nucleation of the Ni-P alloy film. EN plating process requires activation energy in order to trigger the reactions. This energy is supplied in the form of heat. The energy required by the system is one of the most important factors affecting the kinetics or rate of the deposition process (Ref 5).

As mentioned before, the temperature supplies energy for the endothermic reaction of electroless plating and plays an

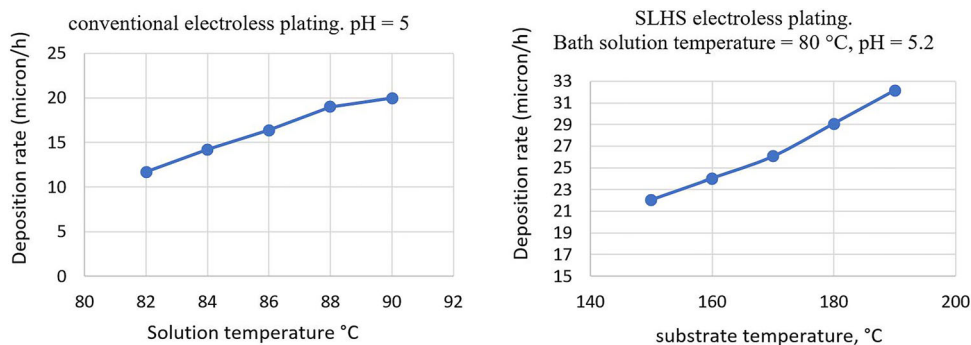


Fig. 2 Comparing the rate of electroless deposition for conventional(left) and SLHS (right) methods

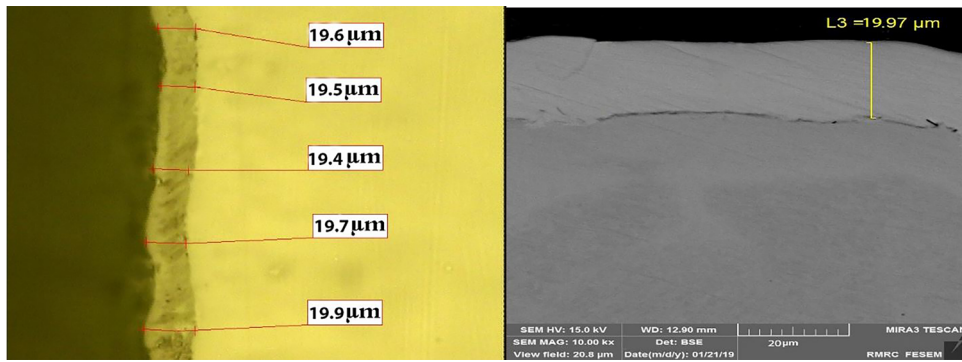


Fig. 3 Result of thickness measurement of the coating via SEM (right) and LM (left) for conventional sample (1 h)

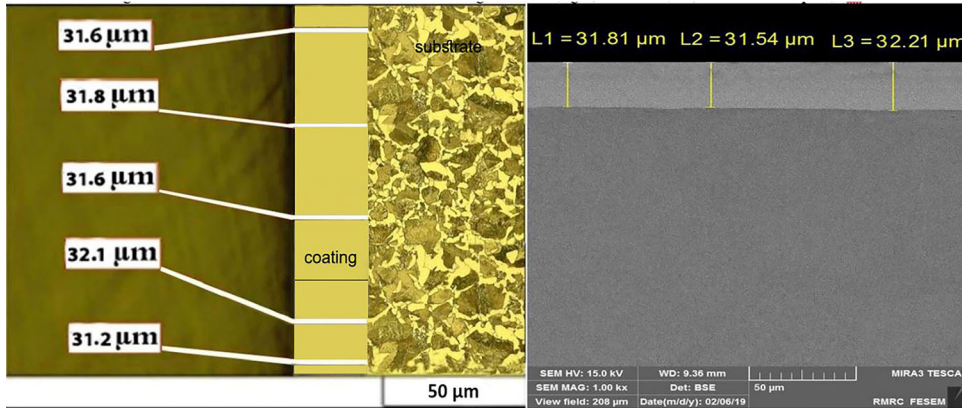


Fig. 4 Result of thickness measurement of the coating via SEM (right) and LM (left) for SLHS sample (1 h)

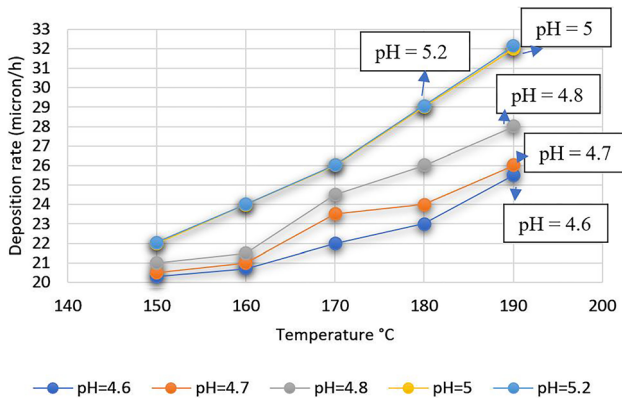


Fig. 5 Plots of deposition rate versus increasing substrate temperature in various pHs for SLHS method

important role as the driving force of processes. In addition, the kinetics of electroless plated Ni-P alloy film is controlled by thermal energy. Increasing the temperature causes a rise in nickel and a drop in phosphorus content in the coating. In fact, in comparison to phosphorus, the deposition rate of nickel is dominated and causes the retardation of the phosphorus deposition process.

3.2 Thermal Simulation of SLHS Method

The thermal simulation of SLHS system was done using two simulation software, namely Abaqus and COMSOL (Fig. 7).

The simulation shows the thermal distribution of heating around the sample and heater. The hottest and the coldest zones of the SLHS method are shown in red and blue, respectively. The combination of heat transfer modes (convection + conduction + radiation) plays a major role in heating up the sample.

3.3 Characterization of Surface Morphology and Microstructure

The morphologies of electroless nickel coatings have been studied in the as-plated condition and after heat-treatment at 400 °C for 1 h utilizing FE-SEM/SEM and LM. As shown in Fig. 8-11, for both methods, Ni-P electroless coating has a spherical grains morphology arranged side by side forming a cauliflower-like characteristic (Ref 26). This kind of morphology also called Broccoli-like or Orange-peel is the specification of Ni-P electroless coating. The size of these spheres depends on the precipitation rate and thickness of Ni-P electroless coating. The possible reason for the formation of such morphology is the tendency to reduce the surface energy of Ni-P precipitates. It was reported that the size of these spheres increases with an increase in coating thickness (Ref 5). The coating seems very dense and uniform.

EDS analyses of Ni-P coating and the percentage of Ni and P for both methods are shown in Fig. 12. It can be seen, for both methods, that the phosphorus content is above 10 wt.%. Based on the amount of P, Ni-P electroless can be categorized in three types:

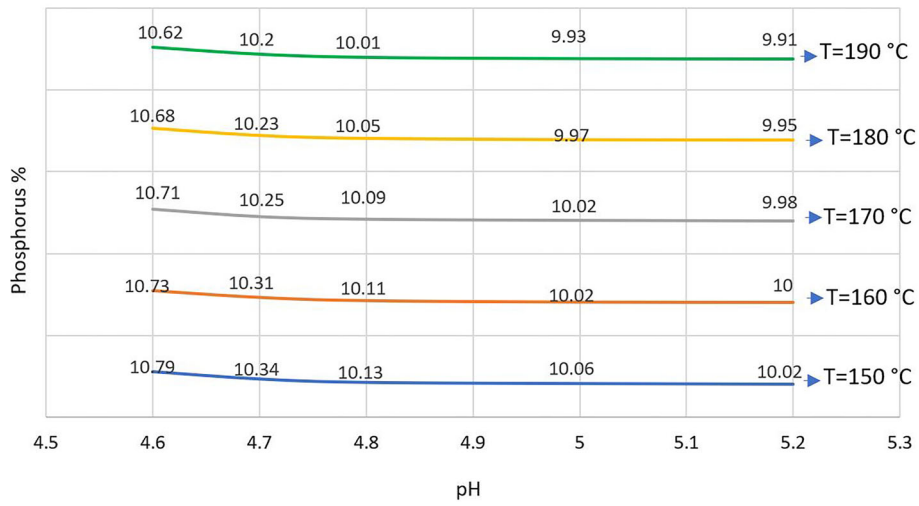


Fig. 6 Plots of phosphorus content versus pH in different substrate temperature for SLHS method

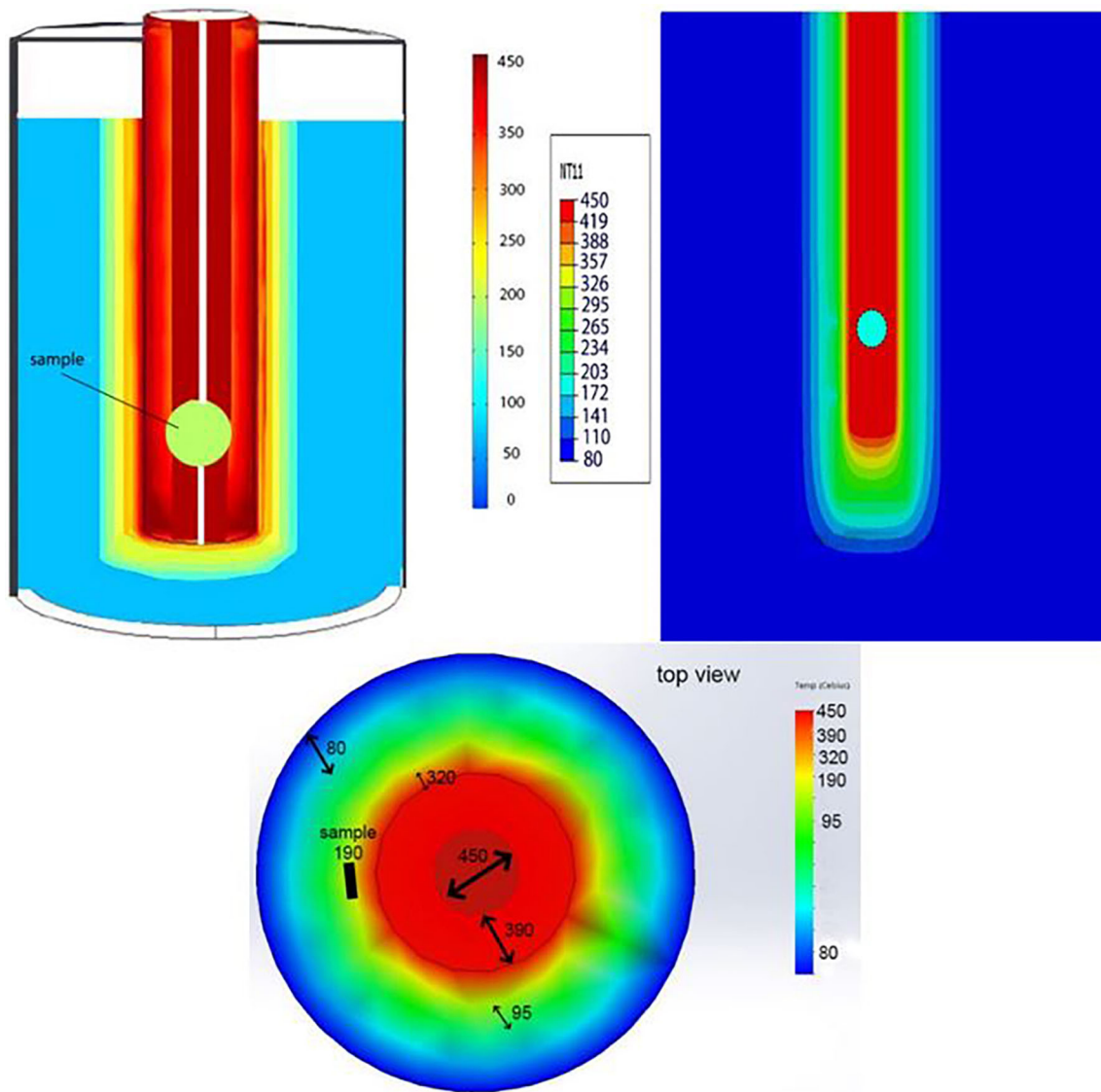


Fig. 7 Schematic illustration of thermal simulation using COMSOL (left) and Abaqus (right) software

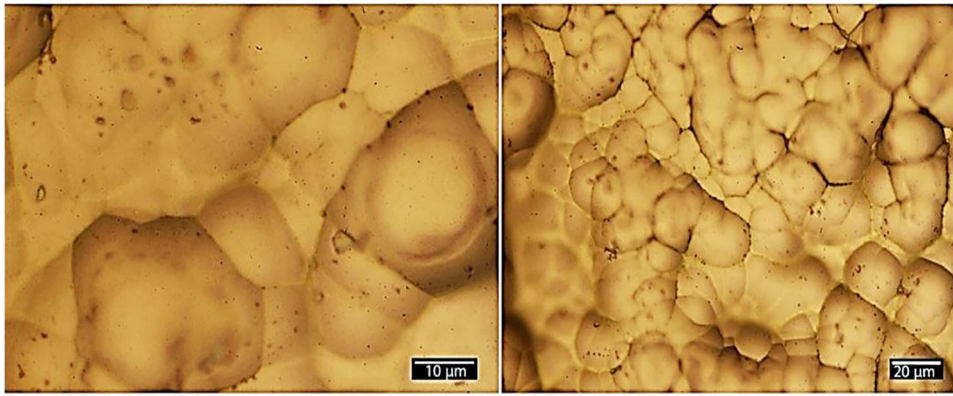


Fig. 8 Light microscopy images of the conventional electroless nickel coating surface

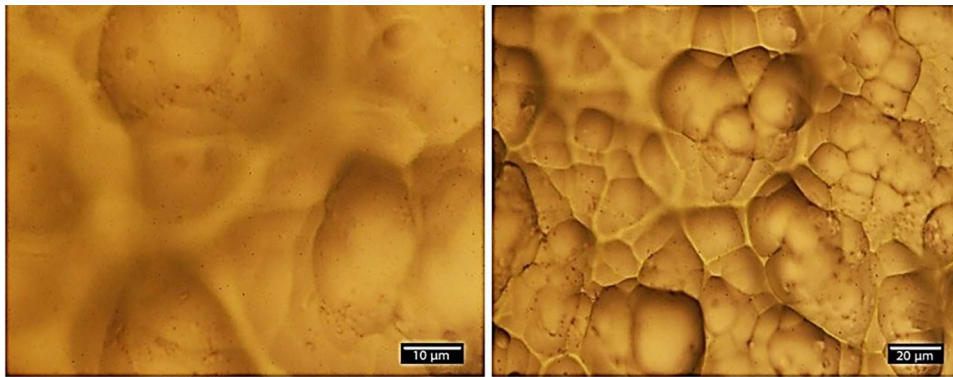


Fig. 9 Light microscopy images of SLHS electroless nickel coating surface

- Low phosphorus (1-5 wt.% P)
- Medium phosphorus (6-9 wt.% P)
- A high phosphorus (10-15 wt.% P)

Each type has its own microstructure. Low P is nano-crystalline, high P has an amorphous microstructure, and the medium group has a mixed nano-crystalline-amorphous structure. Therefore, in this study, coatings structure in the as-plated condition is amorphous because of phosphorus > 10 wt.%. Moreover, for SLHS method the phosphorus content is lower than the conventional one. The possible reason can be related to the high rate of deposition that causes an increase in the Ni content. Generally, the Ni formation reaction is faster than the P formation reaction.

3.4 Phase Analyses

The XRD analysis of the coating pre-heat treatment step is shown in Fig. 13. As shown in figure, in as-plated condition an amorphous wide peak in about 45 °C for both methods appears, and no sharp peak appears in as-plated condition.

After heat-treatment at 400 °C for 1 h, the sharp peaks appeared showing that crystallization happened (Fig. 14). The crystallization is related to the precipitation of stable phases such as f.c.c nickel and b.c.t nickel phosphide phase (Ni₃P). The reason for the formation of such intermetallic (Ni₃P) is the tendency of the materials to decrease their energy. It means the energy level of the Ni₃P compound is lower than either Ni or P elements. This change requires enough energy (heating) to

overcome an activation energy barrier supplied via heat-treatment. X-ray studies of heat-treated deposits showed that Ni(α), Ni₃P, and various meta-stable phases (Ni₇P₅ and Ni₁₂P₅) were present in deposits produced by SLHS method. On the other hand, for conventional samples, Ni(α), Ni₃P, and meta-stable phases (Ni₅P₂ and Ni₇P₅) are present.

The other important point is the presence of peripheral orientation in XRD pattern considering the main peak of Ni. The angles (2θ) for three main peaks of nickel are 44.49°, 51.85° and 76.38°. By changing the plating approach, it can be seen that the sharp peaks, namely Ni (111) and Ni (200) for SLHS graph have higher intensity in comparison to the conventional one. By considering the ratio of intensities between Ni peaks in both approaches, this result can be obtained: conventional : $\left(\frac{I_{Ni(111)}}{I_{Ni(200)}}\right) = \frac{300}{100}$

$$SLHS : \left(\frac{I_{Ni(111)}}{I_{Ni(200)}}\right) = \frac{85}{100} \cdot \frac{\left(\frac{I_{Ni(111)}}{I_{Ni(200)}}\right)_{CON} - \left(\frac{I_{Ni(111)}}{I_{Ni(200)}}\right)_{SLHS}}{\left(\frac{I_{Ni(111)}}{I_{Ni(200)}}\right)_{CON}} \approx 0.72.$$

It means the height of peaks (count) changes about 72%, which may be related to the nature of growth and existence of texture in SLHS method.

3.5 Microhardness Result

Microhardness measurements were made on both kinds of electroless Ni-P samples (conventional and SLHS) in as-plated and after heat-treatment conditions and in unusual pH (3.5). Figure 15 shows the results.

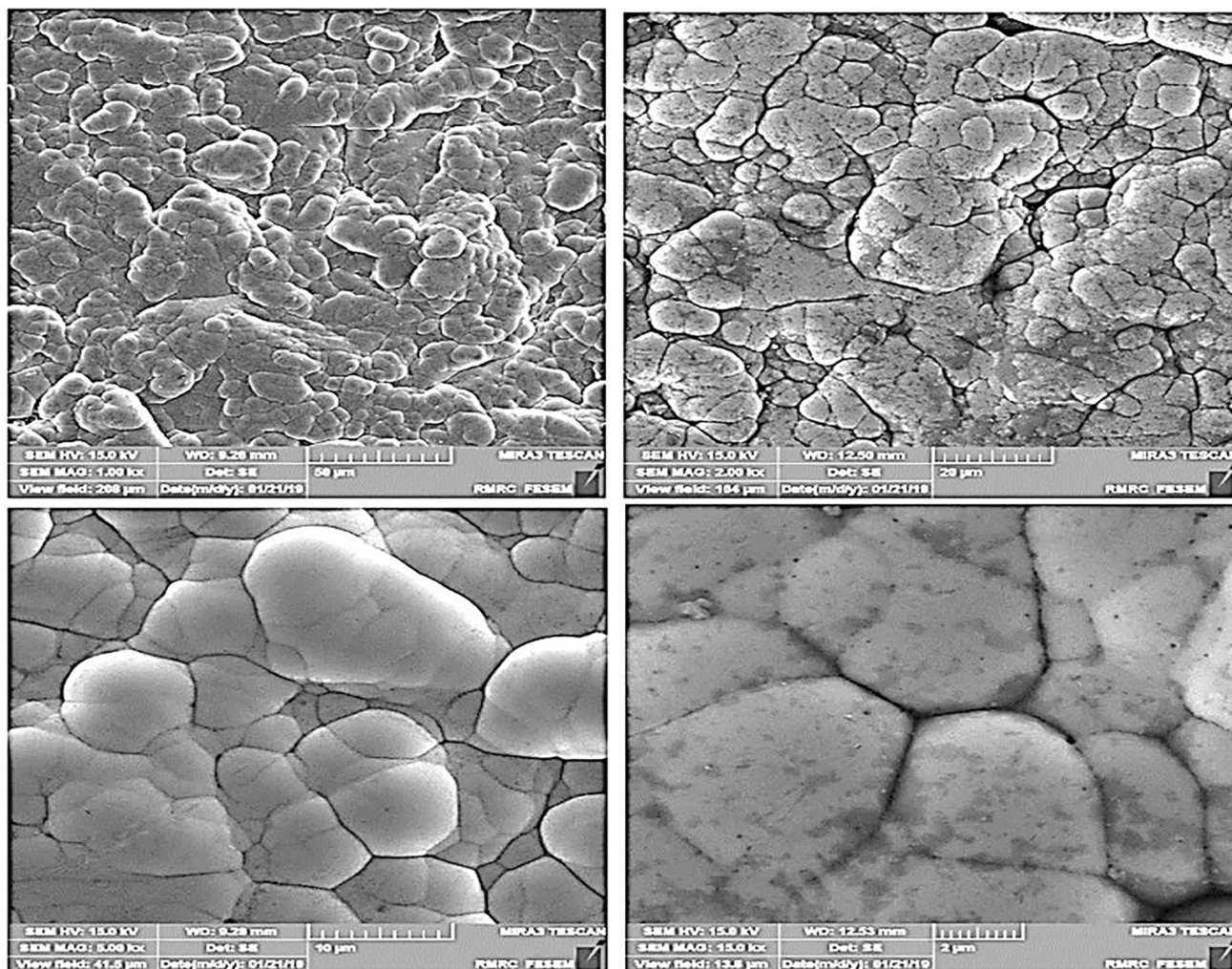


Fig. 10 FE-SEM micrograph of the electroless nickel coating surface (conventional samples) at various magnifications

In general, three factors including phosphorus content, heat-treatment's temperature and time have an effect on the hardness of electroless coatings. The hardness value of electroless coatings, in as-deposit and heat-treatment condition is totally different. In an as-plated condition, by decreasing the phosphorous content, the hardness is increased. After heat-treatment the high phosphorus coatings at 400 °C for 1 h, the hardness increased remarkably, which is attributed to the transformation of the Ni-P phase to Ni₃P (bct) and nickel (fcc). Therefore, the greater formation of the nickel phosphides due to heat-treatment causes an increase in hardness. In the as-plated condition, the hardness of SLHS sample is higher than that in the conventional one because of lower phosphorous content. However, after heat-treatment, again the hardness of SLHS sample is greater than that of the conventional sample. It seems that the hardness of the electroless coating is affected by other factors such as the size and distribution of Ni₃P particles. It is evident from grain size measurement done for Ni and Ni₃P by Scherrer equation that the average size of Ni₃P for SLHS samples is finer than that of the conventional ones (Table 4). Hence, this issue may be the main reason for the appearance of such behavior in SLHS samples.

3.6 Corrosion Test Result

The corrosion resistance of electroless Ni-P coating depends on several factors such as phosphorus content, thickness, porosity and adhesion.

3.6.1 Salt Spray Test. To compare the corrosion resistances, all samples are exposed to an accelerated corrosion test called salt spray for 96 h. The results shown in Tables 5 and 6 indicate that the SLHS sample can provide better protection than the conventional one. Since the pre-treatment processes of the samples were the same, the corrosion behavior of the samples seems to be more related to phosphorus content and thickness of the coatings. The phosphorus content of SLHS samples is less than that of the conventional samples, but the SLHS thickness is more than conventional. Therefore, it seems that in this condition, thicker coatings provide better corrosion resistance. The samples' appearances after this test are shown in Fig. 16.

3.6.2 Open-Circuit Potential Test. Before carrying out, Tafel polarization and EIS tests, the Open-Circuit Potential (OCP) of samples were measured until this potential varies with time scarcely. The result is shown in Fig. 17.

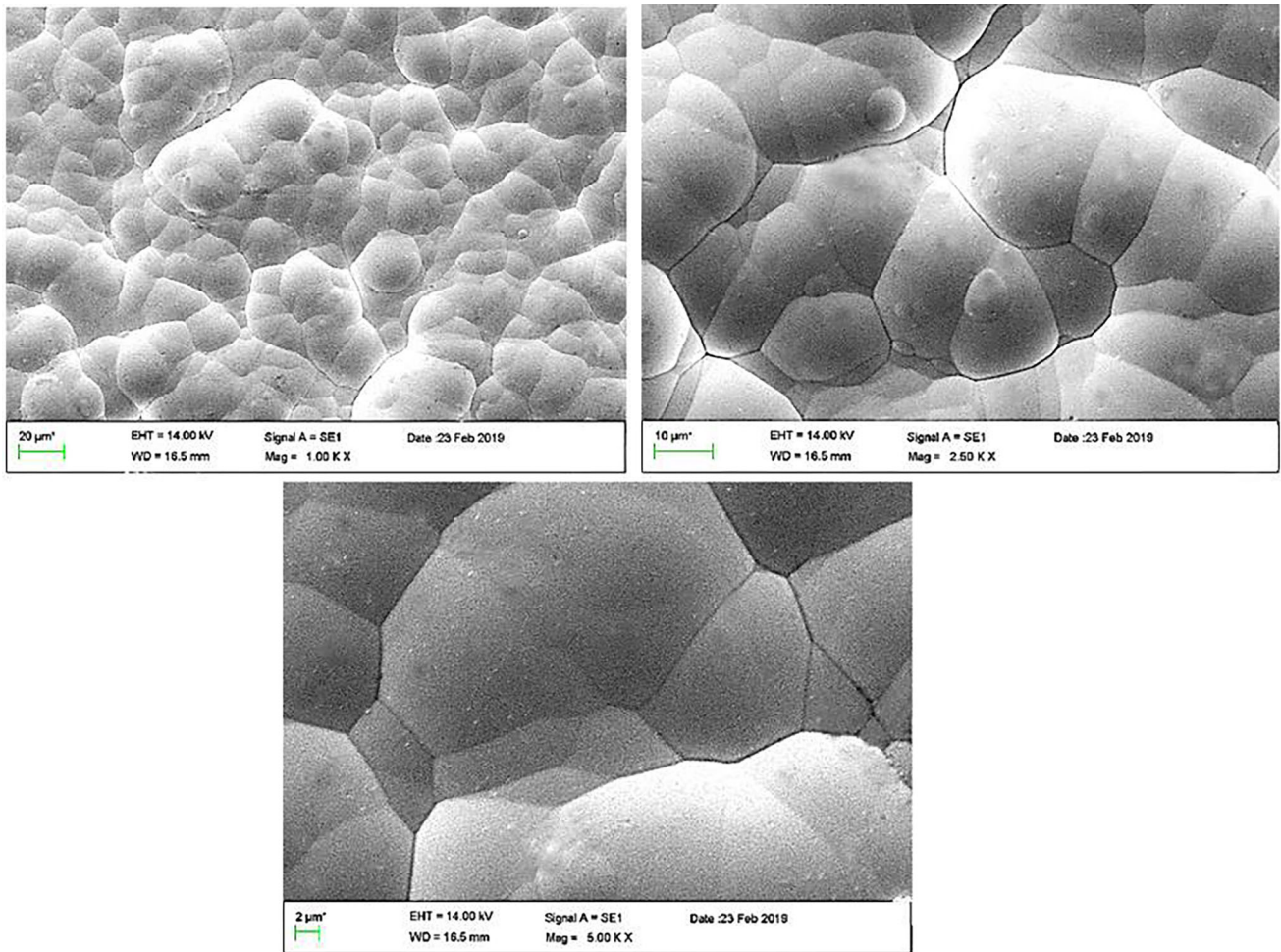


Fig. 11 SEM micrograph of the electroless nickel coating surface (SLHS samples) at various magnifications

3.6.3 Tafel Polarization. Tafel polarization curves for Ni-P electroless coatings in 3.5 wt.% sodium chloride solution for both types of coatings (SLHS and conventional) are shown in Fig. 18. Corrosion current density and corrosion potential quantities are extracted from these curves via extrapolating the linear portions of curves as shown in Table 7. These results show that the SLHS coating has a better corrosion behavior because of more positive corrosion potential and lower corrosion current density. The main reason for this behavior can be related to the increased thickness in SLHS samples in comparison to the conventional one.

3.6.4 EIS Measurement. Figure 19 shows the Nyquist plots of the SLHS and conventional coatings obtained from EIS test. The curves have two semicircles in the high-frequency region just one of which is clear and the other is determinable when the plot is magnified in that region. This indicates that the corrosion process of these coatings is based on a two-time constant behavior. The higher values of charge transfer resistance (R_{ct} or R_p), obtained for the SLHS sample (bigger semi-circle) imply a better corrosion protective ability in comparison to the conventional sample.

The Bode and phase angle plots for SLHS and conventional samples are shown in Fig. 20(a) and (b), respectively. The Bode and phase angle plots show two broad peaks at the analyzed frequency range, which confirms two-time constants behavior. The time constant at lower frequencies is related to

the coating layer, while the time constant corresponding to double layer and charge transfer resistance appear at higher frequencies. According to Bode plots, since the SLHS graph is above the conventional one, it can be concluded that SLHS samples have a better corrosion resistance than the conventional ones.

To evaluate the electrochemical corrosion parameters, the equivalent circuit seen in Fig. 21 is used. Although other kinds of equivalent circuits including two-time constant behavior may be suggested, but this type of equivalent circuit, which gives the best-fitted results with the minimum average error, is chosen. The equivalent circuit simulation program (ZView2) was used for data analysis and fitting. R_s , R_{ct} , and CPE parameters demonstrate solution resistance, charge transfer resistance, and constant phase element, respectively. These parameters were calculated by fitting the EIS data into the circuit model, and the results are shown in Table 8. As shown in Table 8, SLHS coating shows a higher charge transfer resistance in comparison to conventional coating, which is in agreement with the Tafel polarization result. The charge transfer resistance measures the ease of electron transfer across the metal surface, which is inversely proportional to the corrosion rate (Ref 23). This increase in corrosion resistance can again be related to a bigger thickness of SLHS coatings in comparison to conventional ones.

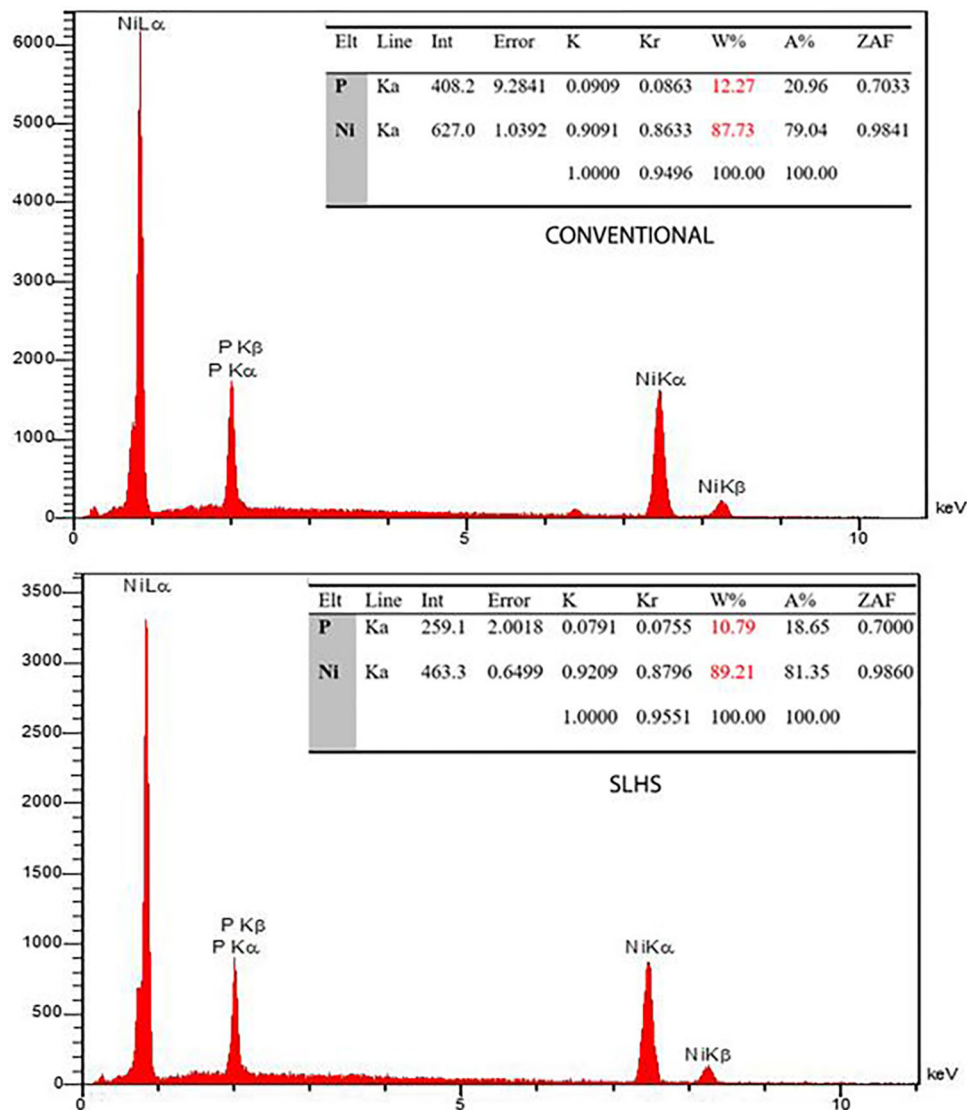


Fig. 12 EDS of Ni-P coating for both SLHS and conventional samples

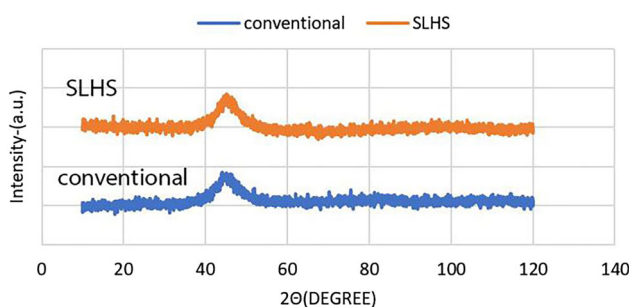


Fig. 13 XRD analysis of Ni-P coating for both SLHS and conventional samples in an as-plated condition

In general, the coating resistance measures the barrier performance of a coating against electrolyte penetration, and the coating capacitance indicates the diffusion of electrolyte solution into the coating. The high coating resistance and the low capacitance, mean higher electrolyte penetrating resistance and lower electrolyte diffusion into the coating, respectively (Ref 23). The equivalent circuit of Fig. 21 contains two

constant phase elements. The first constant phase element (CPE1) is related to the coating capacitance, and the second constant phase element (CPE2) is associated with the double-layer capacitance. The presence of a constant phase element in an equivalent circuit represents a deviation from ideal capacitance behavior because of the inhomogeneity of the surface. The impedance of CPE is given by the following expression: $Z_{CPE} = [Y_0 (j\omega)^n]^{-1}$ (Ref 23), where Y_0 is CPE constant, j depicts an imaginary number ($j^2 = -1$), ω stands for angular frequency (rad s^{-1}) and n illustrates the exponent of CPE and is associated with the micro-roughness and inhomogeneity of the surface, respectively. The capacitance values of the double layer and the coating in the equivalent circuit of Fig. 21 can be calculated from the following equation: $C = [(Y_0 \cdot R)^{1/n}] / R$ (Ref 24). The corresponding values of Y_0 and R for calculating the double-layer capacitance and the coating capacitance are extracted from Table 8. In Table 9, the double-layer capacitance and the coating capacitance of conventional coating and SLHS coating are compared.

According to Table 9, the capacitance values of SLHS samples are smaller than those of the conventional sample.

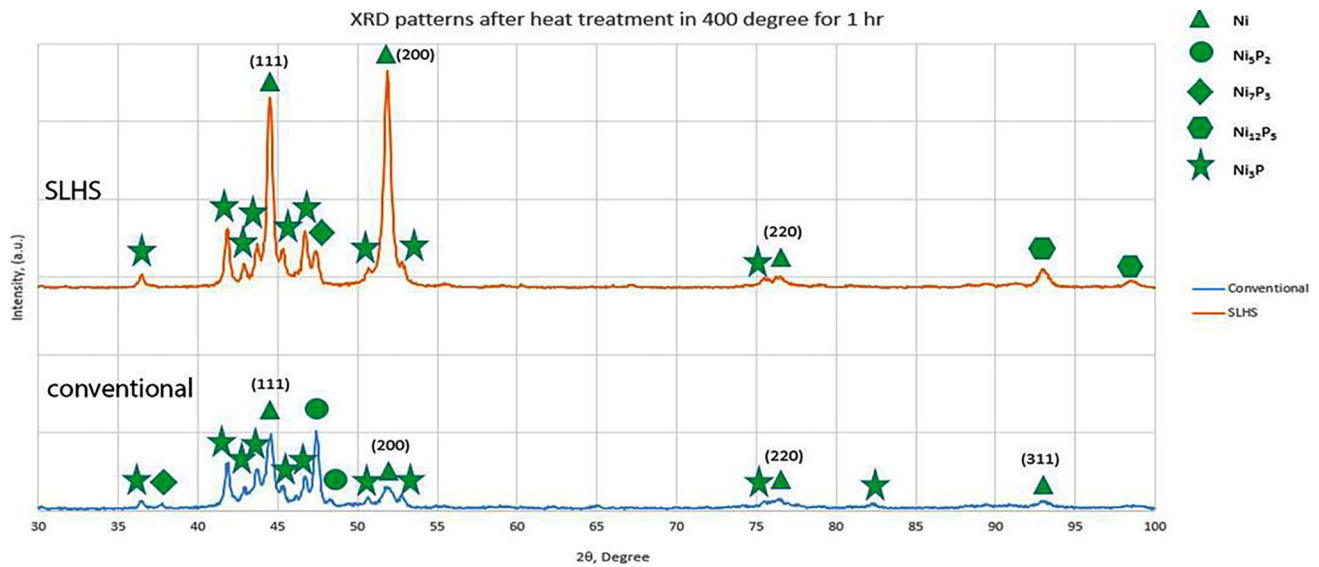


Fig. 14 XRD patterns of Ni-P coating for both SLHS and conventional samples after heat treatment at 400 °C, 1 h

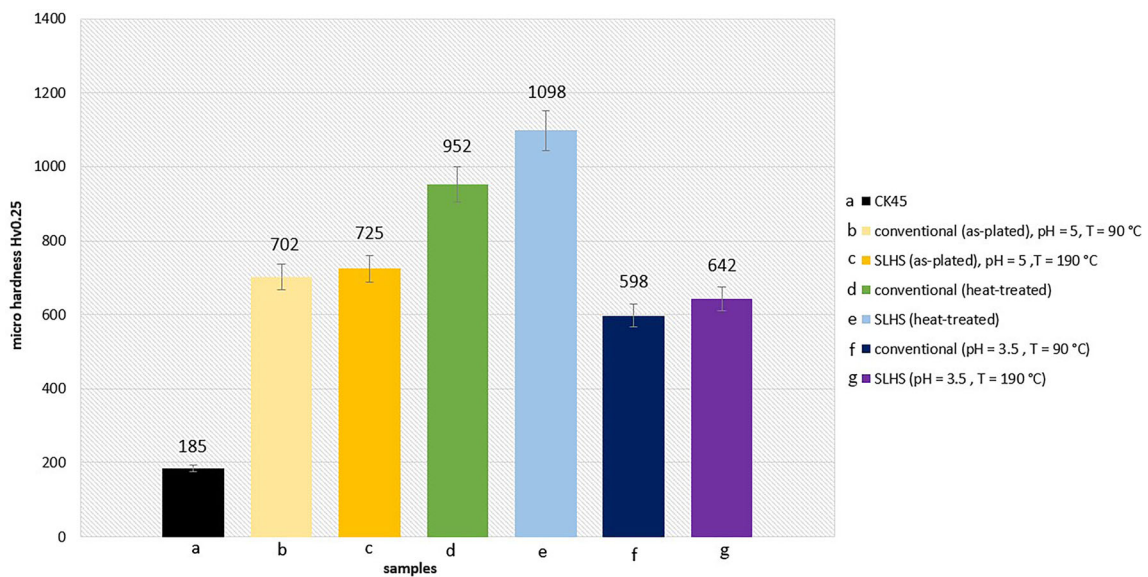


Fig. 15 Comparing microhardness of Ni-P coating for both SLHS and conventional samples before and after heat treatment at 400 °C, 1 h

Table 4 Grain size estimation for SLHS and conventional samples via XRD patterns (after heat-treatment) using Scherrer equation

Samples	Ni ₃ P phase	Ni phase	2θ	FWHM-β (deg)	d(nm)	Average, d(nm)
Conventional	(231)	...	41.76	0.253	34	37.5
	(141)	...	46.63	0.211	41	
SLHS	(231)	...	41.76	0.304	28	28.5
	(141)	...	46.63	0.297	29	
Conventional	...	(111)	44.52	0.407	21	19.5
	...	(200)	51.82	0.488	18	
SLHS	...	(111)	44.52	0.382	22	21
	...	(200)	51.82	0.432	20	

Therefore, it can be said that the barrier properties of the SLHS coating are greater than those of conventional coating.

4. Conclusion

In this work, we have explored a novel method for electroless plating called SLHS and have compared the coating properties with conventional electroless plating. The main results are summarized as follows:

1. Maximum rate of deposition for SLHS method was obtained in this condition: $T_{\text{sub}} = 190\text{ }^{\circ}\text{C}$, $\text{pH} = 5.2$ that was about $32\text{ }\mu\text{m/h}$. The rate for conventional electroless plating was nearly $20\text{ }\mu\text{m/h}$. Therefore, a 60% improvement was observed.
2. The main reasons for boosting the deposition rate in hot substrate method are related to accelerated redox reactions chains of electroless bath in the surface of the sample and combination of heat transfer modes (convection + conduction + radiation).
3. In SLHS technique, the volume of the heating zone near the sample is much smaller than the bath bulk volume.

Table 5 Salt spray results for conventional electroless sample

Symptom observation	Inspection time, h
Few red spots were seen on the surface	24
Red spots increase about 5%	48
Red spots increase about 7%	72
Red spots increase about 10%	96

Table 6 Salt spray results for SLHS electroless sample

Symptom observation	Inspection time, h
Few red spots were seen on the surface	24
Red spots increase about 1%	48
Red spots increase about 2.5%	72
Red spots increase about 3%	96

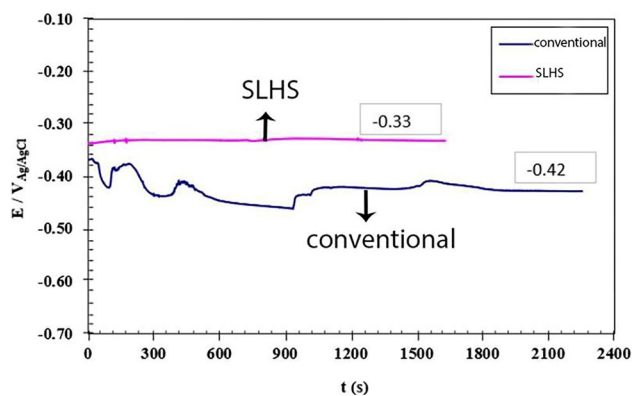


Fig. 17 The OCP test values for both SLHS and conventional plating samples

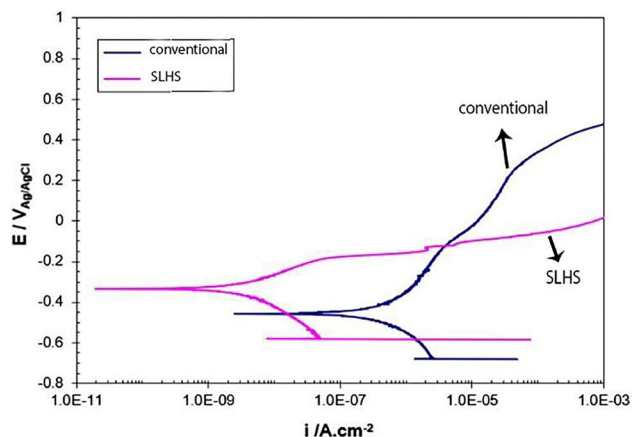


Fig. 18 Tafel polarization curves for SLHS and conventional samples

Table 7 i_{corr} and E_{corr} results for conventional and SLHS electroless samples

Coating	i_{corr} , A/cm^2	E_{corr} , mV
Conventional Ni-P	5.67×10^{-7}	- 0.456
SLHS Ni-P	3.1×10^{-9}	- 0.333

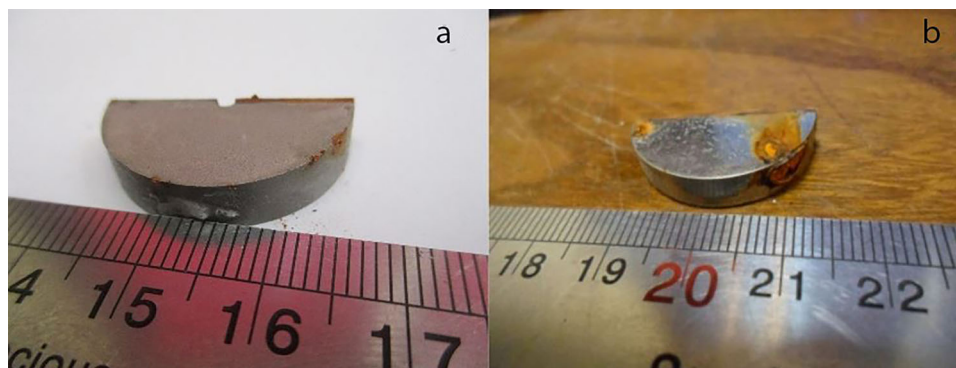


Fig. 16 Samples' appearances after salt spray test for 96 h. (a) SLHS, (b) conventional

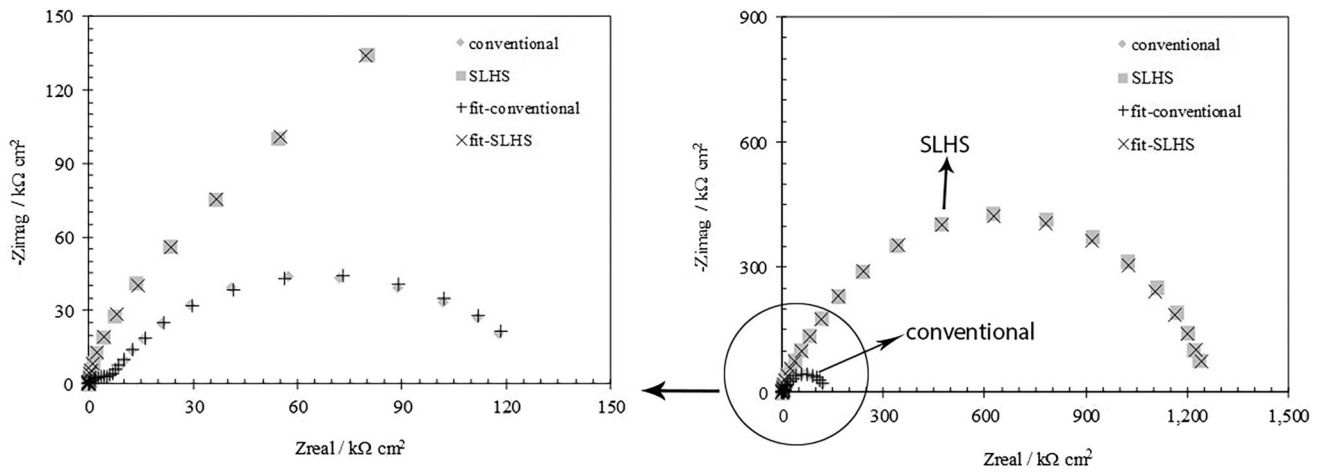


Fig. 19 Nyquist plots of the SLHS and conventional coatings plus their fitting results

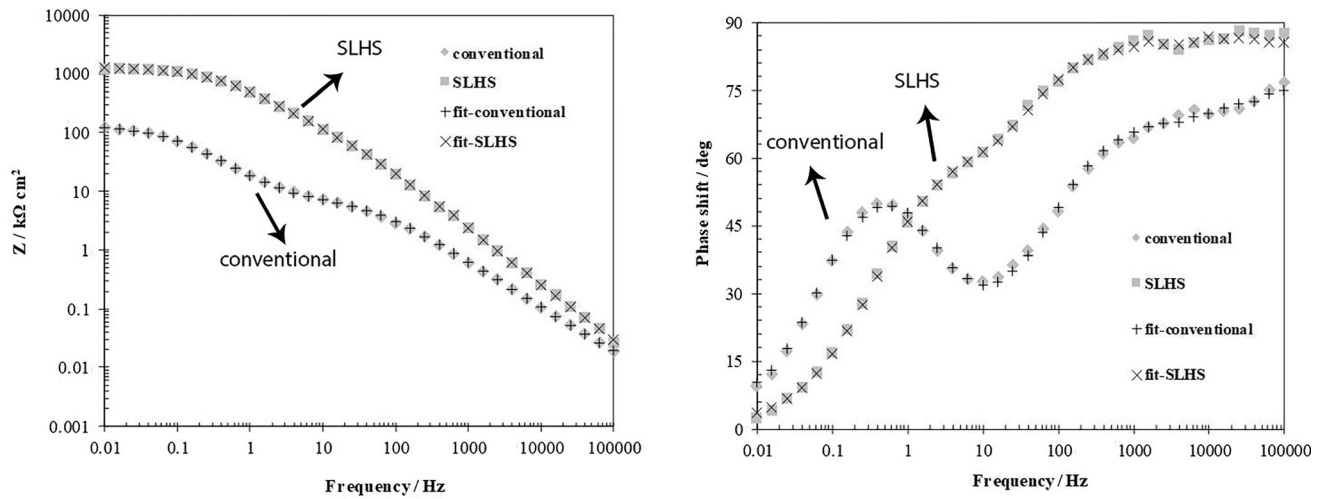


Fig. 20 Bode (left) and phase angle (right) plots for SLHS and conventional samples plus their fitting results

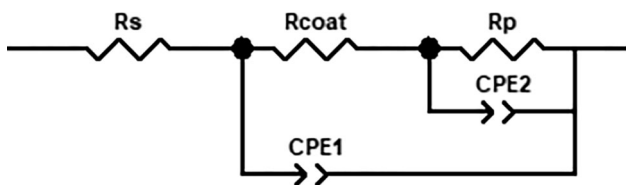


Fig. 21 The equivalent circuit used to obtain the electrochemical corrosion parameters from EIS results for SLHS and conventional samples

Table 9 Capacitance values for the conventional and SLHS electroless samples

Coated samples	C_{coat} , $\mu\text{F}/\text{cm}^2$	$C_{double\ layers}$, $\mu\text{F}/\text{cm}^2$
Conventional Ni-P	0.486	15.560
SLHS Ni-P	0.038	0.327

Table 8 The electrochemical corrosion fitted parameters results for conventional and SLHS electroless samples

Coated samples	R_s , Ω/cm^2	$R_1 = R_{Coat}$, $\text{k}\Omega/\text{cm}^2$	Y_1 (coated), $\mu\Omega^{-1}\text{cm}^{-2}\text{s}^n$	$R_2 = R_P = (R_{CT})$, $\text{k}\Omega/\text{cm}^2$	Y_2 , $\text{dl}, \mu\Omega^{-1}\text{cm}^{-2}\text{s}^n$	n_1	n_2	Chi square, %
Conventional Ni-P	4.06	123.77	13.471	7.45	1.638	0.780	0.784	0.7
SLHS Ni-P	4.13	1183.45	0.382	105.38	0.101	0.684	0.954	0.1

Furthermore, using cold water continuously pumped around the glass beaker can keep the temperature low enough. For the solution near the hot substrate, with the aid of two air tubes, the temperature would not exceed 95 °C.

4. Increasing the pH value above the 5.3 in the high substrate temperature ($T_{\text{sub}} = 190$ °C) causes instability and bath decomposition for SLHS method, even the solution temperature is kept cold enough.
5. The EDAX result shows that the SLHS sample has a lower phosphorus content in comparison to the conventional one. The reason is the higher rate of nickel deposition in SLHS method.
6. According to the salt spray test, Tafel polarization and EIS measurement, better corrosion behavior for SLHS sample is seen than for the conventional one. The reason is related to the bigger thickness of the SLHS coating.
7. The hardness of SLHS sample in both as-plate and heat-treatment conditions is greater than that of the conventional one. It seems that in addition to the phosphorus content of the coating, the size and distribution of Ni_3P hard particles have an important effect on the hardness values.

References

1. J.K. Pancrecius, S.B. Ulaeto, R. Ramya, T.P.D. Rajan, and B.C. Pai, Metallic Composite Coatings by Electroless Technique—A Critical Review, *Int. Mater. Rev.*, 2018, **63**(8), p 488–512
2. M.Q. Yu, Q. Qiao, F. You, C.L. Li et al., Effect of Temperature on Structure and Corrosion Resistance for Electroless NiWP Coating, *Bull. Mater. Sci.*, 2016, **39**(2), p 519–523
3. M. A. Azmah Hanim and L. Vijayaraghavan, Electroless Plating as Surface Finishing in Electronic Packaging, *Comprehensive Materials Finishing*, 2017, Vol 3, p 220–229
4. C.A. Loto, Electroless Nickel Plating—A Review, *Silicon*, 2016, **8**(2), p 177–186
5. W.P. Wu and J.J. Jiang, Effect of Plating Temperature on Electroless Amorphous Ni-P Film on Si Wafers in an Alkaline Bath Solution, *Appl. Nanosci.*, 2017, **7**, p 325–333
6. S.H.M. Anijdan et al., The Effect of Electroless Bath Parameters and Heat Treatment on the Properties of Ni-P and Ni-P-Cu Composite Coatings, *Mater. Res.*, 2018, **21**(2), p 97
7. R. Taheri, *Evaluation of Electroless Nickel-Phosphorus (EN) Coatings*, University of Saskatchewan, Ph.D. Thesis, 2003
8. O.O. Ajibola, D.T. Oloruntoba, and B.O. Adewuyi, Effect of Processing Parameters on the Protective Quality of Electroless nickel-phosphorus on Cast Aluminium Alloy, *J. Metall.*, 2015, **2015**, p 1–12
9. F.E.T. Heakal and M.A. Maamoum, Role of Some Plating Parameters in the Properties of Ni-P/ Al_2O_3 Nanocomposite Coatings on Mg Alloy, *Int. J. Electrochem. Sci.*, 2016, **11**, p 7198–7215
10. A.J. Cobley, J.E. Graves, B. Mkhlef, Ultrasonically Enabled Low-Temperature Electroless Plating for Sustainable Electronic Manufacture, in *4th Electronic System-Integration Technology Conference*, 2012
11. S.R. Anvari, *Deposition, Investigation and Comparison of Mechanical Properties of Nanostructured- Amorphous Ni-P Electroless Hybrid (Functionally Graded and Multilayer) and Monolayer Coatings*, Ph.D Thesis, Isfahan University of Technology, 2016
12. S. Karthikeyan and L. Vijayaraghavan, Study on the Mechanical Properties of Heat-Treated Electroless NiP Coatings Reinforced with Al_2O_3 Nano Particles, *Metall. Mater. Trans. A*, 2016, **47**(5), p 2223–2231
13. C. Gao et al., Electrochemically Promoted Electroless Nickel-Phosphorous Plating on Titanium Substrate, *Appl. Surf. Sci.*, 2017, **392**, p 912–919
14. Y. Sung et al., A Simultaneous Annealing Effect During High-Temperature Electroless Copper Plating Using the Non-isothermal Deposition Method, *Mater. Lett.*, 2008, **62**, p 4461–4463
15. Y. Sung and M. Der Ger, The Behaviors of a Stabilizer in an NITD System with Electroless Nickel Plating, *J. Chin. Inst. Chem. Eng.*, 2003, **34**, p 531–538
16. Y. Sung et al., Novel Route to Deposit Metallic Dot Array or Thin Film on the Conducting and Insulating Substrates, *J. Mater. Sci. Lett.*, 2003, **22**, p 1515–1518
17. Y. Sung et al., Electroless Copper Deposition by Non-isothermal Deposition Technology, *J. Mater. Chem. Phys.*, 2009, **113**, p 303–308
18. Y. Sung et al., Self-assembled Nickel-Phosphorus Micro-dot Arrays Deposited by Non-isothermal Deposition Method, *J. Alloys Compd.*, 2008, **453**, p 407–412
19. Y. Sung et al., Ultrathin Ni-Mo-P Diffusion Barriers Deposited Using Non-isothermal Deposition Method in Acid Bath, *Electrochem. Solid-State Lett.*, 2008, **11**, p D30–D33
20. Y. Sung et al., A Novel Process of Electroless Ni-P Plating by Non-isothermal Method, *Mater. Chem. Phys.*, 2005, **89**, p 383–389
21. W. Riedel, *Electroless Nickel Plating*, Cambridge Scientific Abstracts, 1991
22. M. Fang et al., Electroless Plating and Growth Kinetics of Ni-P Alloy Film on SiCp/Al Composite with High SiC Volume Fraction, *Trans. Nonferrous Met. Soc. China*, 2016, **26**, p 799–805
23. L. Fan et al., Corrosion Resistance of Transmission Pipeline Steel Coated with Five Types of Enamels, *Acta Metall.*, 2017, **30**(4), p 390–398
24. Z. Feng et al., Passivity of 316L Stainless Steel in Borate Buffer Solution Studied by Mott-Schottky Analysis, Atomic Absorption Spectrometry and x-ray Photoelectron Spectroscopy, *Corros. Sci.*, 2010, **52**, p 3646–3653
25. ISO 4527, *Metallic coatings—Autocatalytic (electroless) Nickel-Phosphorus Alloy Coatings—Specification and Test Methods*, International Organization for Standardization, 2003
26. F.E.T. Heakala, M.A. Shoeib, and M.A. Maamoum, Optimizing Parameters Affecting Electroless Ni-P Coatings on AZ91D Magnesium Alloy as Corrosion Protection Barriers, *Prot. Met. Phys. Chem. Surf.*, 2017, **53**(1), p 177–187

Publisher's Note Springer Nature remains neutral with regard to jurisdictional claims in published maps and institutional affiliations.